iJRASET
International Journal For Research in Applied Science and Engineering Technology

INTERNATIONAL JOURNAL FOR RESEARCH

IN APPLIED SCIENCE & ENGINEERING TECHNOLOGY

Volume: 4 **Issue:** IX **Month of publication:** September 2016

DOI:

www.ijraset.com

Call: 08813907089 | E-mail ID: ijraset@gmail.com

Volume 4 Issue IX, September 2016
ISSN: 2321-9653
International Journal for Research in Applied Science & Engineering Technology (IJRASET)

Exfoliated Graphite Fortified MgO-C Refractories

Pradeep Ramawat Sadh[1], Rahul Lodha[2], Kuldeep Singh[3], Vandana Singh[4]
[1,2,4]*Mewar University, Gangrar, Chittorgarh 312901, Rajasthan, India*
[3]*Govt. College of Engineering & Technology, Bikaner 334004, Rajasthan, India*

Abstract— MgO-C refractories have found the wide range of applicability in basic oxygen furnace, electric arc furnace and in steel ladle, due to good thermal shock resistance and improved slag-corrosion resistance at elevated temperature. The slag penetration and corrosion resistance are improved by the formation of dense layer of MgO on the working surface of MgO-C brick, developed due to oxidation of Mg, which can be produced via the reaction between MgO and carbon. However, carbon suffers from poor oxidation resistance and thus may oxidize to form CO and CO_2 resulting in a porous structure with poor strength and corrosion resistance, if this phenomena is not prevented. In this study, reduction of the carbon content while improving the physical and mechanical properties and oxidation resistance of magnesia-carbon refractories. In the present work, we used fabricated exfoliated graphite through microwave treatment as carbon source to replace flaky graphite. In order to study the effect of the replacement on the characteristics of the refractory, the physical and mechanical properties are analysed here in. Magnesia-carbon refractory batches fortified with various fractions of exfoliated graphite have been prepared to understand how the new compositions respond in terms of properties as compared to the available magnesia-carbon refractories. Our aim is to achieve improved properties, along with reduction in carbon burn-out, in the fortified magnesia-carbon refractories.

Keywords— refractories, exfoliated graphite, fortified magnesia ceramics, oxidation resistance, thermal shock resistance

I. INTRODUCTION

Refractories [1], of all kinds, are generally defined as non-metallic inorganic material, with very high melting temperature, outstanding mechanical properties both at room temperature and at high temperatures; and high resistance to withstand rapid temperature fluctuations, including repeated heating and cooling. Most of these materials are also known to have good corrosion and erosion resistance to molten metal, glass, slag and hot gases, etc. Due to good thermal stability of refractories, they are used in kilns, furnaces, boilers, incinerators and other applications in various industries including iron and steel, non-ferrous metal, glass, cement, chemicals, ceramics, etc. MgO-C brick is a composite material based on MgO and C and bonded by high carbon containing pitch and resin [2], with some metallic powder as anti-oxidants to protect the carbon.

These MgO-C bricks are made by high pressure and are of unburned type. These are known to possess excellent resistance to thermal shock and slag corrosion at elevated temperatures. Thus, these materials have found extensive applications in steel making processes especially in basic oxygen furnaces, electric arc furnaces, lining of steel ladles, etc.

MgO-C bricks have the following features:

MgO-C refractories have high refractoriness as no low melting phase occurs between MgO and C.

Graphite, the carbon source, has very low thermal expansion; hence in the composite of MgO-C the thermal expansion is low.

Graphite has very high thermal conductivity, which imparts high thermal conductivity in the MgO-C composite.

Thermal shock resistance of MgO-C is very high because the thermal expansion is low and the thermal conductivity is high.

MgO-C bricks prevent the penetration of slag and molten steel because of the non-wettability of carbon.

MgO-C refractories are able to absorb stress, thus keeping down the amount of discontinuous wear due to cracks.

II. EXPERIMENTAL WORK

A. Raw Materials

Commercially available high quality with low impurity fused magnesia (FM), natural flakes graphite, aluminium metal powder (-150 µm), boron carbide powder and expanded graphite were used to maintain the granulometry of the mixture. Liquid resin and

resin powder were taken as additives of base raw materials for the fabrication of low carbon graded MgO-C brick. As mentioned earlier, this research work is focused on the preparation of exfoliated graphite [4] to use in MgO-C refractory as partial replacement of graphite.

In this present work, high purity magnesia was taken as the raw material for fused magnesia, considering the selection criteria like purity, CaO/SiO_2 ratio, low Fe_2O_3 content and large crystals in the range of 500-1500 µm. [2, 3] High purity graphite was taken as a raw material for carbon and resin was used as binder. The chemical properties of magnesia, flake graphite and liquid resin are given in the tables below.

TABLE I
Chemical Composition of Fused Magnesia

Raw material/ Wt. %	MgO	Al_2O_3	SiO_2	CaO	Fe_2O_3	Na_2O
Fused magnesia	97.10	0.07	0.40	1.40	0.50	0.50

TABLE II
Chemical Analysis of Flake Graphite

Material/ Wt. %	Carbon	Volatile Matter	Ash
Flake Graphite	97.05	0.69	2.26

TABLE III
Physical and Chemical Analysis of Liquid Resin

Properties	Liquid resin
Viscosity (CPS) at 25°C	8500-9000
Specific gravity at 25°C	1.2g.cm^{-3}
Non-volatile matter (%)	80
Fixed carbon (%)	48
Moisture (%)	~5

TABLE IV
Effect of Microwave Energy on the C-Axis Exfoliation of Graphite.

Energy (W)	c-axis elongation (nm)
1000	56
900	64
800	74
700	58

1) Preparation Of MgO–ExG Composite Powder: In order to distribute the ExG homogeneously in magnesia powders, the as-prepared ExG and MgO powders were mixed for 15 min in a steel container rotating at a speed of 400 rpm with silicon nitride balls as the abrasive media. The mixing ratio of magnesia powder to ExG was 6.70:1. The composite powder obtained was designated as

MgO–ExG.

2) Fabrication Of MgO-C Brick: The composite material prepared as above, was used to replace a part of the graphite phase for the preparation of a limited number of MgO-C refractory bricks.

3) Batch Preparation: Different batches of MgO-C brick were prepared by taking the same amount of MgO, resin and anti-oxidant contents. However, different compositions of MgO-C bricks will be fabricated using different amounts of exfoliated graphite as partial replacement of the natural flake graphite. All the variations done in the study are to be compared with the conventionally used MgO-C brick composition [5, 6, 7], prepared under similar conditions.

TABLE V
Carbon Component in Magnesia-Carbon Bricks

Carbon content (Wt. %)	B1	B2	B3	B4	B5
Normal Graphite	5.0	4.5	4.0	3.0	2.5
Exfoliate Graphite	0.0	0.5	1.0	2.0	2.5

3) Mixing: The purpose of mixing the raw materials is to make a refractory batch and transform all the solid components and the liquid additions into a macro homogeneous mixture that can be subsequently moulded or shaped by one of the numerous fabrication methods employed by modern refractory manufacturers. All the above batches were separately mixed in a pan mixer at room temperature for a period of 45 minutes. All the solid raw materials and liquid additives are mixed in a sequence to get a macro homogeneous mixture. The following table shows the mixing sequence of various raw materials.

TABLE VI
Mixing Sequence Followed for Manufacture of Magnesia-Carbon Bricks

Steps	Sequence of mixing	Mixing time (min)
1	Course and medium MgO grains + graphite + Al metal powder + B_4C powder + resin powder	5
2	Liquid resin	10
3	Previously mixed MgO-ExG powder & fine MgO powder	30

4) Aging: After homogeneously mixing of the materials, the batches were kept for 2 hour for ageing. During aging the polymerization of resin takes place by developing carbon-carbon bonds.

5) Pressing: The mixed materials after aging were compacted to give a desired shape by pressing. The aged mixtures will be pressed uniaxial by hydraulic press in a steel mould of internal dimension 230*115*89 mm 20W40 lubricating oil (Indian Oil Corporation). An appropriate weight of each mixture will be taken to get the desired green density and the size of the brick. The mixtures have to be charged slowly into the mould cavity and leveled uniformly in order to avoid lamination in the pressed bricks.

6) Tempering: Tempering is the heat treatment process of the refractories at low temperature to remove volatile matters from the organic green binders and to impart enough green strength for handling [3, 8]. By this process the chemical bond is developed in the refractory grains and the bonding phase. Tempering of the pressed green bricks is to done at 230°C for 2-12 hours. With the increase in temperature phenolic resin got converted to carbonaceous phase, which help in developing a stronger carbonaceous bond for the refractory brick and increased the mechanical strength of the brick.

B. Characterizations and Measurement Techniques

1) TG Analysis: Thermal analysis of the samples is to be carried out primarily to determine the oxidation temperature of graphite and also to measure the amounts of residue, which has been assumed to the quantity of silicon carbide contained in each of the samples prepared in this investigation. For this purpose, a small quantity of the sample will be subjected to TGA in flowing air atmosphere with a heating rate of 5°C/minute.

2) Apparent Porosity (AP) and Bulk Density (BD): AP is defined as ratio of the total volume of the closed pores to its bulk volume and expressed as a percentage of the bulk volume. Closed porosity is the pores that are not penetrated by the immersion liquid, whereas open porosity are those pores which are penetrated by the immersion liquid. AP was measured as per the standard of IS: 1528, Part-8 (1974) both for tempered and coke samples. The Archimedean evacuation method generally measures both bulk density and apparent porosity.

3) Cold Crushing Strength (CCS): Cold crushing strength of refractory bricks and shapes is the gross compressive stress required to cause fracture. The cold crushing strength of the tempered and coked samples was measured as per ASTMC-133. The test samples were cut from the standard brick samples. Cold crushing strength of the refractories is measured by placing a suitable refractory specimen of on flat surface followed by application of uniform load to it through a bearing block in a standard mechanical or hydraulic compression testing machine. The load at which crack appears in the refractory specimen represents the cold crushing strength of the specimen. The load is applied uniformly on the sample in the flat position. It is expressed as kg/cm^2.The working formula for calculating CCS is given by CCS = Load/Area (kg/cm^2)

4) Modulus of Rupture: Modulus of Rupture (MOR) was determined by the conventional three-point bending test conforming to ASTM standards, using MOR testing apparatus. All the specimens for MOR testing are dried at 110°C after wet cutting, without pre-firing in air atmosphere. For modulus of rupture, the tests were carried out at room temperature and the heating rate for Hot MOR testing was 5°C/min and the final firing temperature is 1300°C in air atmosphere with a soaking time of 30 min. The loading rate for both hot and room temperature MOR was 0.15MPa/sec.

5) Oxidation Resistance: Oxidation resistance of the fabricated bricks was tested on cube shaped samples. The samples were fired in an electrical furnace at 1400°C for 10 hours in air atmosphere. At this temperature all the carbonaceous materials of the brick got oxidized particularly from the outer surface. The colour of the oxidized portion turned off-white compared to the black colour of the virgin brick and therefore the boundary between the un-oxidized and the oxidized regions were quite evident. After the heat-treatment, the cuboid shaped samples were cut and the diameter of black portion was measured at different locations and the average value was taken.

Oxidation index is determined by the formula:

$$\text{Oxidation index} = (\text{Area of oxidized zone} / \text{Total area}) \times 100$$

Lower oxidation index indicates the higher oxidation resistance of the brick.

It may be noted that conventionally the oxidation resistance tests are carried out by firing the samples at 1400°C for 5 hours. However we have used a much more stringent test standard for measuring oxidation resistance of our specimens.

6) Thermal Shock Resistance: Thermal shock/thermal spalling is the direct result of exposing the refractory installations to rapid heating and cooling conditions which cause temperature gradients within the refractory. Such gradients cause an uneven thermal strain distribution through the sample, may cause failure of the material. The standard method of finding out spalling resistance is heating the material at an elevated temperature followed by sudden cooling in air at ambient temperature. The thermal shock resistance of refractory materials is determined using standard quench tests in which the material is heated and cooled subsequently and the number of heating and cooling cycles that a material can withstand prior to failure is taken as its thermal shock resistance. The quantification is done by the number of cycles to withstand such temperature fluctuations. The sample specimens cut from tempered bricks. These samples are heated at 1200ºC for 10 minutes and then suddenly brought down to ambient conditions by cooling it in the air for 10 minutes. The number of cycles before any crack in the specimen will be noted down as the thermal shock resistance.

III. RESULTS AND DISCUSSION

Structure and chemistry of graphite and expanded graphite are depicted below:

Volume 4 Issue IX, September 2016
ISSN: 2321-9653
International Journal for Research in Applied Science & Engineering Technology (IJRASET)

A. Phase Analysis & TGA Analysis

Predominantly, a hexagonal structure with confirmed peaks at location a, c and d in the XRD patterns existed in natural graphite with approximately 2% rhombohedral structure as calculated from minor peak "b". This rhombohedral structure could not be distinguished or recalculated in the X-ray diffraction pattern of exfoliated graphite due to overlap in "b" and "c" peaks, but the broad area in the over lab indicated that both hexagonal and rhombohedral peaks were present, however calculating the residual amount resulted in numerous iterations on the software and the values were not consistent to the 3-sigma rules. An investigation of natural graphite was done by using different experimental techniques like SEM and XRD. Natural graphite was characterized were characterized from the points of view of their particle size, crystallinity, purity etc. From SEM images it was observed that natural graphite is flaky in nature and the graphene layers are attached together and that the dimension of graphite flakes is more than 200 µm.

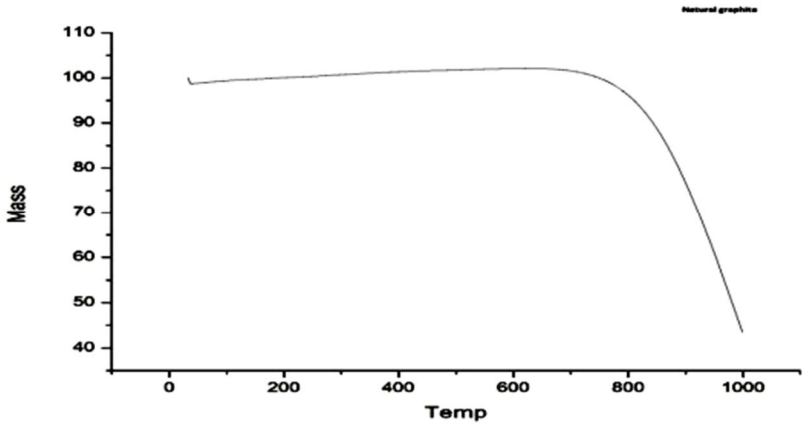

Fig. 1 Thermal analysis of the natural flake graphite sample

Thermal analysis was done in flowing air atmosphere up to a temperature of 1000°C at 10°C/min. Results of TGA analysis of natural flake graphite samples are presented in Fig. 1. As expected severe oxidation took place and consequently weight loss occurred. However, the process was not complete up to 1000°C (weight didn't become constant). Still from the graph we can have an idea that almost 85-90% graphite was oxidized at that temperature range. From the SEM images of expanded graphite it was clear that the natural graphite was expanded. After exfoliation the graphite flakes are expanded perpendicular to the graphene layers and gives a warm like structure. Spacing between the graphene layers increased up to 30 µm.

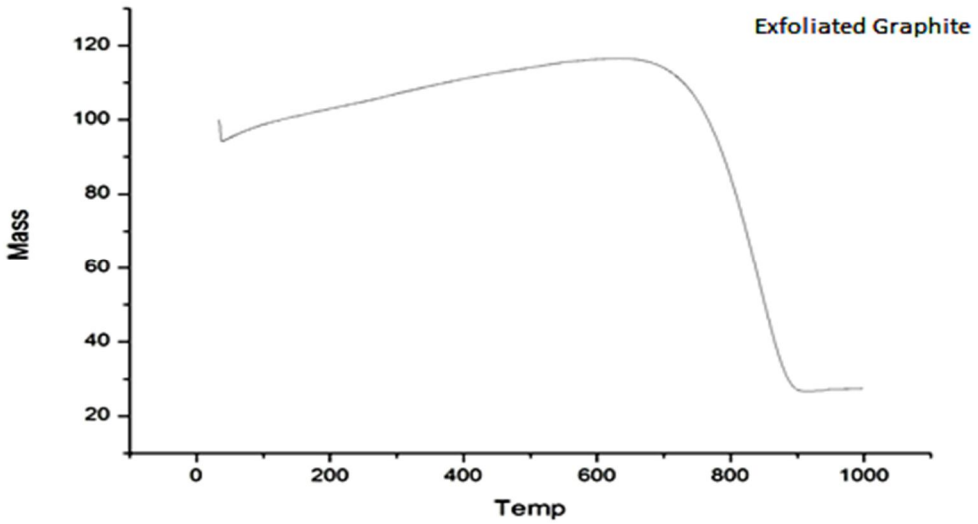

Fig. 2 Thermal analysis of the exfoliated graphite sample

Volume 4 Issue IX, September 2016
ISSN: 2321-9653
International Journal for Research in Applied Science & Engineering Technology (IJRASET)

Conditions of thermal analysis were same as the natural graphite. Results of TGA analysis of natural flake graphite samples are presented in Fig. The result is almost similar to the natural graphite. But the weight loss started at lower temperature due to high reactivity of expanded graphite. The oxidization process was completed around 900°C. From the CHN test, the carbon percentage present in the expanded graphite and other constituents are shown in table VII.

TABLE VII
Weight Percentage of Carbon, Hydrogen & Nitrogen in Exfoliated Graphite

Weight % of Element	Carbon	Hydrogen	Nitrogen
Expanded graphite	73.56	4.47	2.14

XRD pattern of exfoliated graphite is similar to the natural graphite except some extra impurity peaks which came due to the presence of manganese oxide. There's a lot of difference in the peak intensities. Natural graphite shows a great, sharp and symmetrical peak shape because of its high crystallinity. After oxide intercalation, crystal defects increase. As a result crystallinity decrease and diffraction peak intensity decrease.

Physical properties of the prepared magnesia-carbon bricks before and after coking are described below.

Apparent Porosity and Bulk Density (before coking)

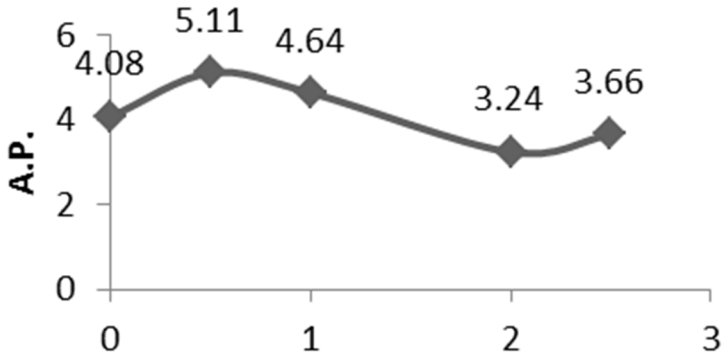

Fig. 3 Variation of apparent porosity with the variation of exfoliated graphite content

With the addition of expanded graphite the percentage of AP is reducing. The AP varies in the range of 3.02 to 5wt%.AP has the value of 4.1 without any expanded graphite and has the value 3 for 0.8wt% exfoliated graphite.

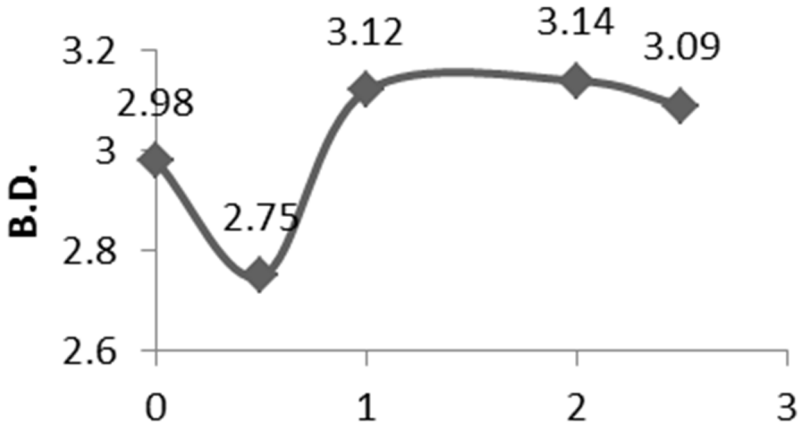

Fig. 4 Variation of bulk density with the variation of exfoliated graphite content

Volume 4 Issue IX, September 2016
ISSN: 2321-9653
International Journal for Research in Applied Science & Engineering Technology (IJRASET)

The variation of bulk density is shown in fig. The variation of bulk density with the exfoliated graphite is very less which ranges from 2.91 g.cm^{-3} to 3.05 g.cm^{-3}. The bulk density without the exfoliated graphite was 2.95 g.cm^{-3}.

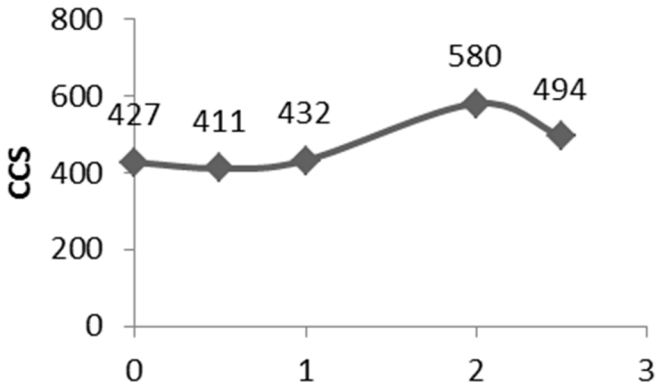

Fig. 5 Variation of cold crushing strength with the variation of exfoliated graphite content

Increase in CCS is because of the increase of exfoliated graphite which causes better filling of pores and results inan increase in BD. But at 0.8 wt% of exfoliated graphite best pore filling is achieved. So, further addition of exfoliated graphite does not affect the CCS value much. Similar trend is seen for MOR as in Fig. 6.

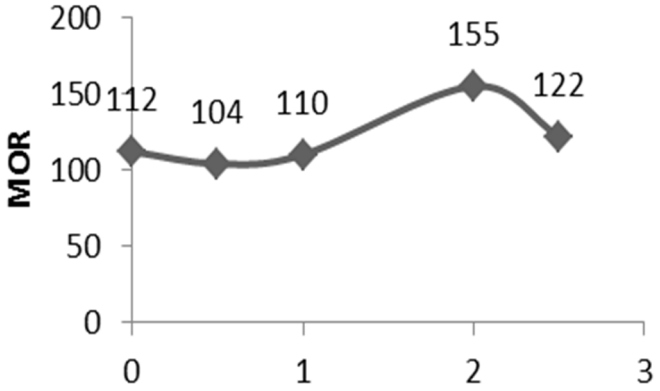

Fig. 6 Variation of modulus of rupture with the variation of exfoliated graphite content

Apparent Porosity, Bulk Density and Cold Crushing Strength (after coking):

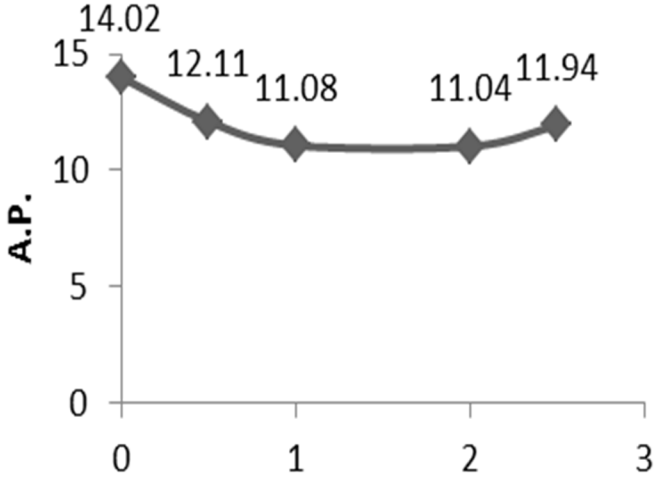

Fig. 7 Variation of coked apparent porosity with the variation of exfoliated graphite content

Volume 4 Issue IX, September 2016
ISSN: 2321-9653
International Journal for Research in Applied Science & Engineering Technology (IJRASET)

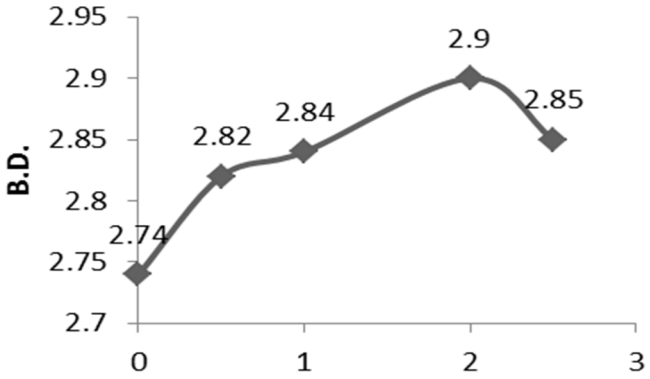

Fig. 8 Variation of coked bulk density with the variation of exfoliated graphite content

The change in bulk density of coked bricks is shown in fig. The values of bulk density vary from 2.84 g.cm^{-3} to 2.91 g.cm^{-3}. The values decrease in comparison with bulk density of tampered bricks.

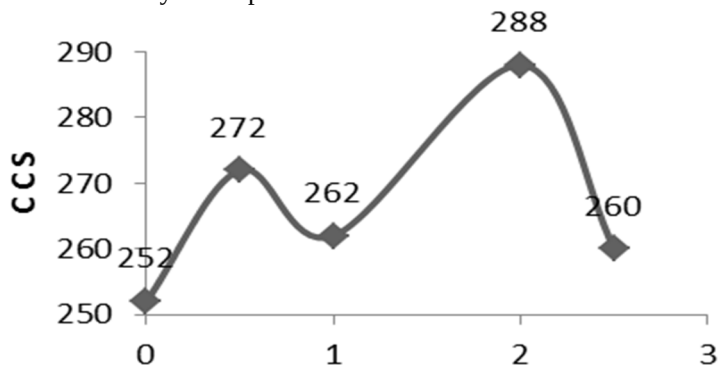

Fig. 9 Variation of cold crushing strength with the variation of exfoliated graphite content

The coked CCS values are shown in fig. 9. The CCS values of coked samples vary in between 174 kg.cm^{-2} to 239 kg.cm^{-2}.

Thermal Shock Resistance

The thermal shock resistance of different samples is shown in fig. 10. Batch 1 which contains no exfoliated graphite shows a good result than batch 2 and 3. Batch 2 and batch 3 shatter after 7th and 8th thermal cycle, whereas the batch 1 and batch 5 samples shatters after 9th thermal cycle. But Batch 4 breaks at 10th thermal cycle. Batch 4 shows better thermal shock resistance than others because as the percentage of exfoliated graphite increases so distribution of carbon into the entire matrix increases.

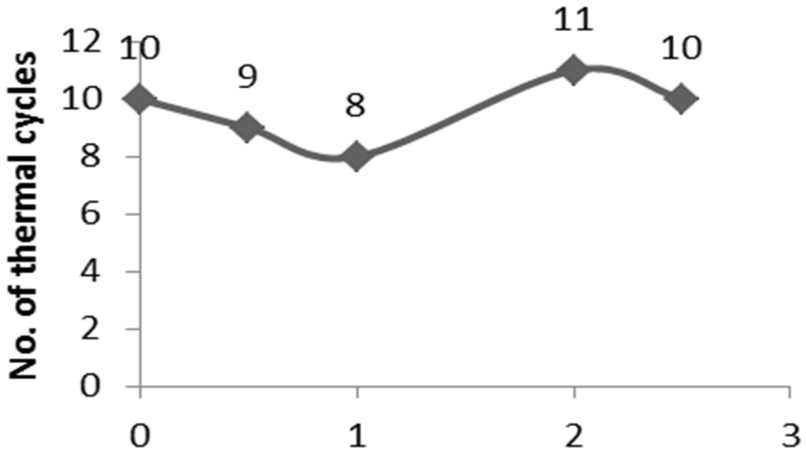

Fig. 10 Variation of number of thermal cycles with the variation of exfoliated graphite content

IV. CONCLUSIONS

The significant features of the new class of refractories fabricated are as follows:

The ExG fortified MgO-C refractories exhibited lower apparent porosity for 2 and 2.5wt% ExG compositions as compared to the standard MgO-C refractory (with no ExG). For these two compositions, bulk density was also found to increase marginally to 3.14 $g.cm^{-3}$ from 2.98 $g.cm^{-3}$ for the standard brick.

The new compositions exhibited a maximum of 35% increase in the cold crushing strength relative to the standard compositions.

Apparent porosity of the coked samples shows progressive lowering in porosity up to 2 wt% with the amount of ExG used, although the coked porosity was higher than uncoked. Additionally, the coked bulk density was found to decrease than the standard composition.

The trend of CCS for coked samples were similar to those of uncoked samples with Batch 4 of the new compositions showing ~14% increase in coked CCS.

Batch 4 exhibited increase in HMOR. The increment was almost 25% higher than that of the standard MgO-C refractory.

The new formulations showed better thermal shock resistance. While the standard brick failed at 10 air quenching cycles, our composition went past 11 cycles.

Dramatic increase in oxidation resistance was observed for the new compositions with an index of ~40% as compared to ~60% for the standard composition.

In totally we have formulated a low carbon MgO-C refractory with 5% graphite with special carbon additives that exhibits excellent thermo-mechanical properties as noted above. Compositions with 0.5, 1 and 2.5 wt% ExG additives had either comparable or slight variation in properties as compared to the standard composition. On the other hand, refractories with 2wt% additives exhibited dramatically improved thermo-mechanical properties including HMOR, thermal shock resistance and oxidation resistance.

REFERENCES

[1] Annual book of ASTM standard, Refractories: Activated carbon, Activated ceramics, 15.01, pp. 19, 2003.
[2] Emad Mohamed M.Ewais, Carbon based refractories, Journal of the Ceramic Society of Japan, vol. 112 pp. 517-532, 2004.
[3] O. Sasan, D. Arash, Micro structure and phase evolution of alumina-spinel self-flowing refractory castables containing nano-alumina particles, Ceramics International vol. 37 pp. 1003–1009, 2011.
[4] G.D.T. Angeles, J.V. Francisco, H.D.A. Antonio, Direct mineralogical composition of MgO–C refractory material obtained by Rietveld methodology, Journal of the European Ceramic Society, vol. 26, pp. 2587–2592, 2006.
[5] X. C. Li, B.Q. Zhu, T.X. Wang, Effect of electromagnetic field on slag corrosion resistance of low carbon MgO–C refractories, Ceramics International vol 38, pp. 2105–2109, 2012.
[6] P. Nicolas, O. Evariste, High temperature mechanical characterization of an alumina refractory concrete for blast furnace main trough Part I. General context, Journal of the European Ceramic Society, vol. 28 pp. 2859–2865, 2008.
[7] W.S. Resende, R.M. Stoll, S.M. Justus ,R.M. Andrade ,E. Longo, J.B. Baldo, E.R. Leite, C.A. Paskocimas, L.E.B. Soledade, J.E.Gomes, J.A. Varela, Key features of alumina/magnesia/graphite refractories for steel ladle lining, Journal of the European Ceramic Society, vol. 20, pp. 1419–1427, 2000.
[8] S. Mucahit, A. Sedat, O. Salih, A micro structural study of surface hydration on a magnesia refractory, Ceramics International vol. 36 pp.1731–1735, 2010.

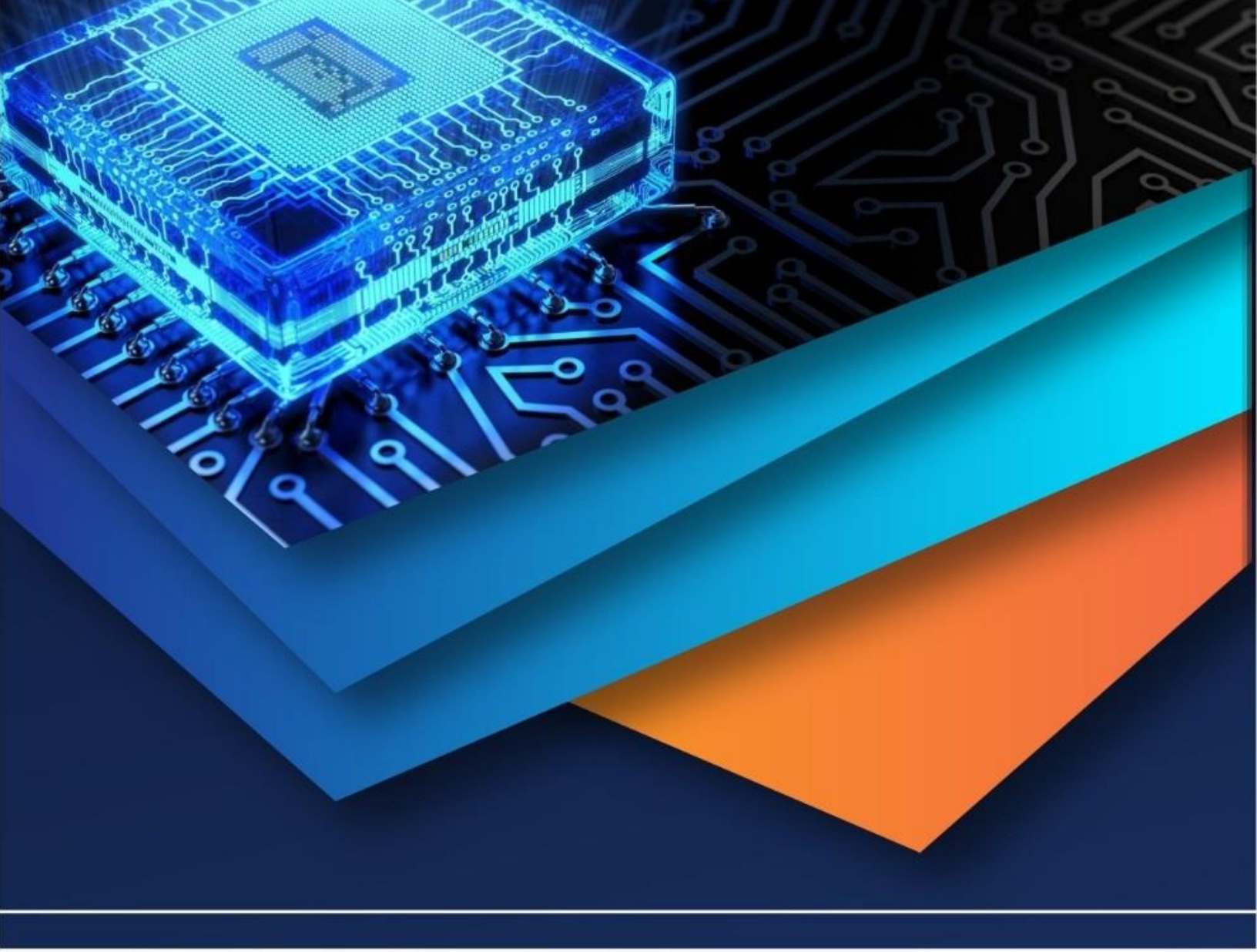

10.22214/IJRASET

45.98

IMPACT FACTOR: 7.129

IMPACT FACTOR: 7.429

INTERNATIONAL JOURNAL FOR RESEARCH

IN APPLIED SCIENCE & ENGINEERING TECHNOLOGY